

Non-reversal and non-repeating quantum walks

K. Barr,¹ T. Proctor,¹ B. Hanson,¹ S. Martiel,^{1,2} V. Pavlovic,^{1,3} A. Bullivant,¹ and V. Kendon¹

¹*School of Physics and Astronomy, E. C. Stoner Building, University of Leeds, Leeds LS2 9 JT*

²*Lab. I3S, CNRS-UMR 7271, BP 121, 06903 Sophia Antipolis cedex, France*

³*Faculty of Science and Mathematics, University of Nis, Serbia*

(Dated: March 29, 2022)

We introduce a variation of the discrete time quantum walk, the non-reversal quantum walk, which is not allowed to step back onto a position which it has just occupied. This allows us to simulate a dimer and we achieve it by introducing a new type of coin operator. The non-repeating walk, which never steps in the same direction as it just stepped in, arises by a permutation of the coin operator. We describe the basic properties of both walks and prove that the joint moments of the non-repeating walker are independent of the initial condition, being determined by five parameters derived from the coin instead. Numerical evidence suggests that the same is the case for the non-reversal walk. This contrasts strongly with previously studied coins such as the Grover operator, where the initial condition can be used to control the standard deviation of the walker.

I. INTRODUCTION

The discrete time quantum walk has been extensively studied since its introduction. Initially, various models were proposed [1–3] with a variety of applications in mind. In this paper we are concerned with the transport properties of a new type of quantum walk. Quantum walks have been shown to have interesting transport properties in a variety of scenarios. On the line they achieve ballistic transport [4] and they were first shown to have an exponential speedup over the classical random walk on the hypercube by Kempe [5]. The faster hitting times have been used in algorithmic applications [5–7].

The quantum walks introduced thus far concern idealised walkers with no spatial extension. Whilst these have many uses in modelling physical and biological processes [8], in some cases we may want to consider walkers which do have spatial extension, and hence cannot move into space which they are already occupying. Self-avoiding random walks were developed to model precisely such processes, initially the folding of polymers. In some cases, such a restricted model may not be suitable. Continuing the example, polymers can overlap to form loops, but they cannot occupy volume that they already occupy. A type of intermediary between the fully random walk and the self-avoiding walk is known as the non-reversal walk. A non-reversing random walker is allowed to occupy spaces on a lattice that it has previously occupied, but is not allowed to return to the point which it has just come from. In this paper we introduce a quantum version of such a walk, which effectively simulates a dimer made up of distinguishable particles, as shown in Figure 1. The motivation for studying such a walk is much the same as that for studying the classical version: more realistic simulation of physical systems.

In both the classical and quantum case, the self-avoiding or non-reversal walk on the line is trivial. This is because there are only two degrees of freedom in the movement, so if one of those is prohibited by the model,

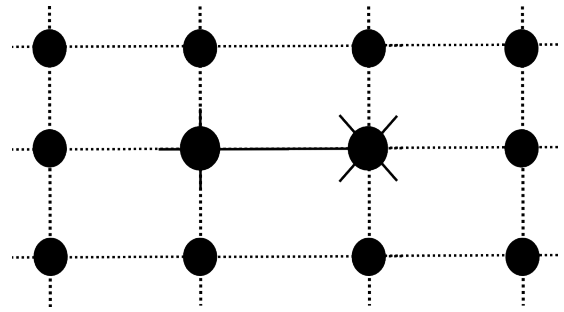


FIG. 1. The head and tail of a dimer on a square lattice, the \times marking the head, and the $+$ marking the tail. As the tail prevents the head moving left, the head can move up, down, or right, resulting in a non-reversing walk

then unidirectional ballistic transport is obtained. The walks studied in this paper take place over a square lattice, in which case the dynamics are highly non-trivial. The paper proceeds as follows: In Section I A classical self-avoiding walks are described in more detail. Then for the sake of comparison the properties of the quantum walk on the square lattice are discussed in Section I B. The non-reversal, and the related non-repeating quantum walk are then defined in Section II. The properties of the non-repeating walk are explored analytically in Section III. With the aid of numerical simulations, the non-reversal walk is investigated in Section IV. We finish in Section V with some concluding remarks.

A. Classical self-avoiding random walks

The classical self-avoiding walk has proven difficult to treat analytically, hence the results concerning it have all so far been numerical [9] and there remain many open questions about it. Even enumerating the number of self-avoiding walks has proven very difficult, despite them being so rare that coming upon one by mistake when examining a random walk is highly improbable.

If c_n is the number of self-avoiding walks of precisely n steps, then the total number of self-avoiding walks up to length n is $\sum_{n \geq 2} c_n$. Some facts are clear, for example that $c_{n+m} \leq c_n + c_m$. The set of self-avoiding walks of length n concatenated with those of length m contains not only the self-avoiding walks of length $n + m$ but some which overlap, hence the inequality. However, determining the precise number of walks is difficult, though bounds have been established. The number of self-avoiding walks must be less than the number of non-reversal walks, as these include the self-avoiding walk as a subset. Additionally it is possible to construct subsets of self-avoiding walks which grow as 2^n , so we know that there are between 2^n and 3^n self-avoiding random walks. The best evidence so far suggests that the number of self-avoiding walks of length n is proportional to 2.638^n , and this is provided as a non-rigorous estimate in [10]. The evidence for this value was obtained by enumerating each such walk of length up to 51 and required a 1024 processor supercomputer [11]. Without new algorithms it is unlikely that we will be able to enumerate much further than this. Guttmann obtained 14,059,415,980,606,050,644,844 walks using this method [11], however these walks make up less than 1 in 360 million of the possible random walks of this length.

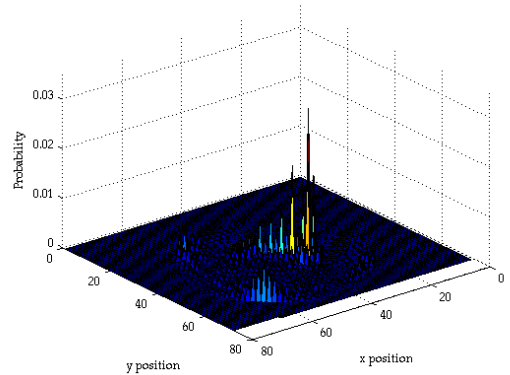
As even counting the walks has proved difficult, it is unsurprising that little is known regarding other properties. The property we are most interested in when comparing walks is the standard deviation. The mean squared displacement is conjectured to be proportional to $n^{3/2}$ though so far, even a proof that the exponent must be between 1 and 2 is elusive [9].

Another known fact about self-avoiding walks demonstrates a key difference between the self-avoiding walk and its standard and non-reversal counterparts. This is that the self-avoiding walk does not necessarily continue indefinitely. This is because it is possible to reach a lattice site whose only adjacent lattice sites have previously been visited, hence the walker cannot continue. After the first few steps there is a small probability that the walk will end on any subsequent step.

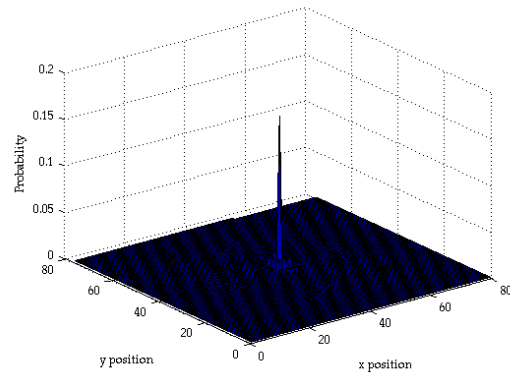
The non-reversal walk is in some ways more tractable. For example, it is clear that on the square lattice there are 3^n such walks, where n is the number of steps traversed by the walker. Its mean squared displacement is $2n$, so it spreads twice as fast as the standard random walk, but slower than the completely self-avoiding walk. There is very little literature on the non-reversal walk, and this tends to examine specific characteristics of the walk relevant to the study of polymer chains [12], rather than its general features.

B. Quantum walks on the square lattice

The properties of the discrete time quantum walk on the square lattice were extensively explored in [13] following initial investigations in [14]. In particular they



a)



b)

FIG. 2. (Color online) Probability distributions arising from a) the DFT coin and b) the Grover coin for the symmetric initial state shown in Equation (6)

examined the mean distance at time t :

$$\langle r \rangle_t = \sum_{x,y} \sqrt{x^2 + y^2} p(x, y, t) \quad (1)$$

where r is the radial distance from the origin, and $p(x, y, t)$ is the probability of finding the walker at position (x, y) at time t . They also characterise the walks in terms of the standard deviation:

$$\sigma = \sqrt{\langle r^2 \rangle - \langle r \rangle^2} \quad (2)$$

The authors use three choices of coin operator. Their first choice behaves like the Hadamard operator for both the 'left/right' ($|l\rangle/|r\rangle$) coin states and the 'up/down' ($|u\rangle/|d\rangle$) coin states:

$$H \otimes H = \frac{1}{2} \begin{pmatrix} 1 & 1 & 1 & 1 \\ 1 & -1 & 1 & -1 \\ 1 & 1 & -1 & -1 \\ 1 & -1 & -1 & 1 \end{pmatrix} \quad (3)$$

This operator does not mix the two dimensions, so a two dimensional version of the distribution of the walk on the line is obtained. More interestingly, they consider the DFT coin operator:

$$D^4 = \frac{1}{2} \begin{pmatrix} 1 & 1 & 1 & 1 \\ 1 & i & 1 & -i \\ 1 & -1 & 1 & -1 \\ 1 & -i & -1 & i \end{pmatrix} \quad (4)$$

and the Grover coin:

$$G^4 = \frac{1}{2} \begin{pmatrix} -1 & 1 & 1 & 1 \\ 1 & -1 & 1 & 1 \\ 1 & 1 & -1 & 1 \\ 1 & 1 & 1 & -1 \end{pmatrix} \quad (5)$$

These operators were tested for a number of initial conditions. These coins are both unbiased, in that they distribute amplitude equally between each coin state. In contrast to the walk on the line, they find that the dynamics of the walk depend strongly on the coin used. Additionally, the dynamics for a specific coin depend strongly on the choice of initial state. The lowest and highest standard deviations obtained for the position of the walker were found using the Grover operator. It was observed that the reason for this is that regardless of the initial state, the distribution forms a central spike, with a ring around it which propagates outwards. The choice of initial condition controls how much probability is situated in the central spike, and how much probability is situated in the ring. The initial state at the origin for both the distributions plotted in Figure 2 is:

$$|\psi\rangle = \frac{1}{2}(|l\rangle + i|r\rangle) \otimes (|d\rangle + i|u\rangle) \otimes |0\rangle \quad (6)$$

The authors of [13] studied all unbiased four dimensional unitary operators with entries equal to either $\pm 1/2$ or $\pm i/2$, which when the leading diagonal is selected to be $1/2$ gives 640 unitary operators. These operators were found to fall into ten types, with the DFT, Hadamard and Grover all being of different type.

II. DEFINITION

We will now define our non-reversal quantum walk on the square lattice. Whilst in the treatment of walks on the square lattice in [13] the specification of the shift operation is implied, more care must be taken here to ensure that the coin operator really does what we want it to. Two variations of the shift, one which shifts amplitude from, say, the ‘moving-right’ state of one node to the ‘moving-right’ state of the next, as is used in [14], and one which shifts amplitude to the opposite end of the edge represented by a given coin state, are considered.

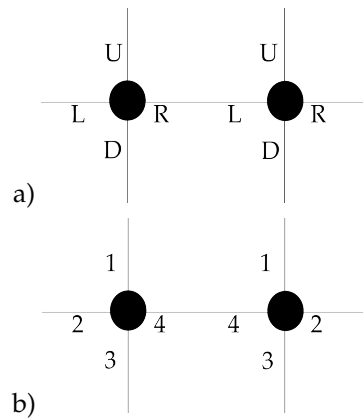


FIG. 3. The two versions of the shift operation correspond to two different coin state labellings: a) each coin state moves amplitude in a specific direction and b) each coin state labels a specific edge on the lattice.

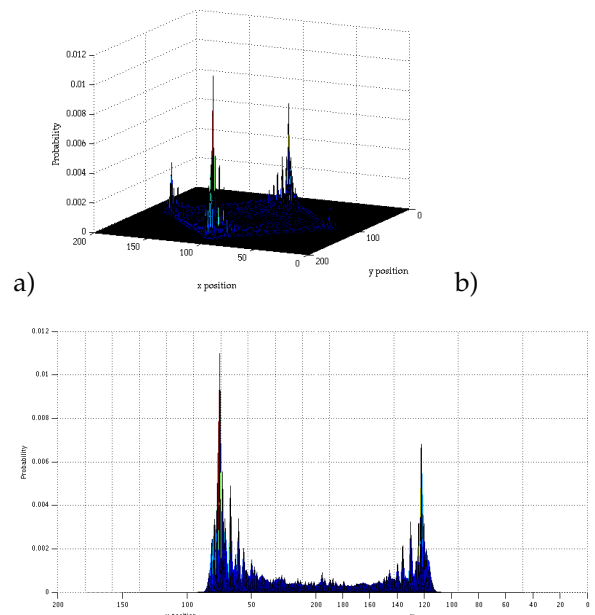


FIG. 4. (Color online) Probability distributions arising after 100 steps of a typical non-reversal quantum walk shown a) over the entire lattice and b) in profile- as the axes are viewed from the corner of the lattice, both x and y positions are visible

The way these two shift operations arise on a lattice is depicted in Figure 3. The non-reversal walk arises when the edge labelling based permutation is used, this is the shift operation defined in [15]. To facilitate the Fourier analysis below, we permute the coin rather than the shift, but the effect on the walk is identical. Whilst the non-reversing walker is a single particle, when interpreted as a dimer it is presumed that the two parts of the non-reversing walker are distinguishable, so one leads the other, as shown in Figure 1.

The state of the walker, Ψ , at time $t \in \mathbb{N}$ is described

by a 4-dimensional vector which is a function of each discrete lattice point $(x, y) \in \mathbb{Z}^2$. We denote this as

$$\Psi(x, y, t) = \begin{pmatrix} \psi_1(x, y, t) \\ \psi_2(x, y, t) \\ \psi_3(x, y, t) \\ \psi_4(x, y, t) \end{pmatrix} \quad (7)$$

$$C^{!rep} = \begin{pmatrix} 0 & \lambda e^{i\alpha} & \gamma e^{i\beta} & f(\lambda, \gamma) e^{i\theta} \\ \lambda e^{-i(\phi+\delta+\alpha)} & 0 & -f(\lambda, \gamma) e^{i(\psi-\theta+\beta)} & \gamma e^{i\psi} \\ -\gamma e^{-i(\delta+\alpha+\psi)} & -f(\lambda, \gamma) e^{i(\phi-\theta+\alpha)} & 0 & \lambda e^{i\phi} \\ f(\lambda, \gamma) e^{i(\theta-\alpha-\psi-\phi-\beta)} & -\gamma e^{i(\delta+\alpha-\beta)} & \lambda e^{i\delta} & 0 \end{pmatrix} \quad (8)$$

where all of the variables are real, $0 \leq \gamma^2 + \lambda^2 \leq 1$, and $f(\lambda, \gamma) = \sqrt{1 - (\lambda^2 + \gamma^2)}$. This is the most general $SU(4)$ operator with zeros on the diagonal. We will also consider

$$C^{!rev} = \begin{pmatrix} 0 & 1 & 0 & 0 \\ 1 & 0 & 0 & 0 \\ 0 & 0 & 0 & 1 \\ 0 & 0 & 1 & 0 \end{pmatrix} C^{!rep} \quad (9)$$

we clearly see that the non-reversing operator $C^{!rev}$ is a permutation of coin operator $C^{!rep}$. The permutations arise naturally when one considers the freedom in choice of edge labelling on a 2d lattice as shown in Figure 3. To define the total time evolution operator, $U^{!rep}$ first define:

$$C\psi(x, y, t) = \begin{pmatrix} \psi_+^x(x, y, t) \\ \psi_-^x(x, y, t) \\ \psi_+^y(x, y, t) \\ \psi_-^y(x, y, t) \end{pmatrix} \quad (10)$$

These values represent the amplitudes at position (x, y) at time t after the coin operation from step $t + 1$. One step of the walk can then be computed by applying both the shift and coin operation:

$$\Psi(x, y, t+1) = U\psi(x, y, t) = SC\Psi(x, y, t) = \begin{pmatrix} \psi_-^x(x+1, y, t) \\ \psi_+^x(x-1, y, t) \\ \psi_-^y(x, y+1, t) \\ \psi_+^y(x, y-1, t) \end{pmatrix} \quad (11)$$

The shift operation as defined here corresponds to the coin state labelling scheme indicated in Figure 3 a).

As the arising walk dynamics have notable properties in common we discuss both. A simple example of a non-reversal coin, used to produce the probability distribution shown in Figure 4, takes $\theta = \phi = \frac{3\pi}{4}$, $\alpha = \beta = \delta = \psi = \frac{-\pi}{4}$ and $\lambda = \gamma = f(\lambda, \gamma) = \frac{1}{\sqrt{3}}$ in $C^{!rev}$. This leads to the following coin:

where we have $\sum_{x,y,i} |\psi_i(x, y, t)|^2 = 1$ and each component is a complex function of discrete position and time. The coin operator will then be given by a unitary in $SU(4)$. The first coin we will consider will be called the non-repeating coin, denoted $C^{!rep}$ as it never allows amplitude to move in the same direction in two consecutive steps. This coin is defined by:

$$C^1 = \frac{e^{-i\frac{\pi}{4}}}{\sqrt{3}} \begin{pmatrix} 1 & 0 & 1 & 1 \\ 0 & 1 & 1 & -1 \\ -1 & -1 & 1 & 0 \\ 1 & -1 & 0 & -1 \end{pmatrix} \quad (12)$$

where the global phase factor can be dropped. An example of a typical probability distribution arising from a non-reversal, or non-repeating quantum walk is shown in Figure 4. The distribution is shown in 2d and in profile in order to show the similarity of the profile to that of the walk on the line. Regardless of initial condition, the dynamics are similar, tracing out a square with peaks at each corner. The initial condition determines the height and number of distinctive peaks at the corners of the square. The initial condition used to obtain the distribution shown in Figure 4 is given by Equation (6).

III. FOURIER ANALYSIS

In order to analytically study the large t behaviour of the quantum walks defined above, we use Fourier analysis. The Fourier transform from position space to momentum space is

$$\hat{\Psi}(k_x, k_y, t) = \sum_{x,y} \Psi(x, y, t) e^{i(k_x x + k_y y)} \quad (13)$$

with the inverse transform given by

$$\Psi(x, y, t) = \int_{-\pi}^{\pi} \int_{-\pi}^{\pi} \frac{dk_x dk_y}{(2\pi)^2} \hat{\Psi}(k_x, k_y, t) e^{-i(k_x x + k_y y)} \quad (14)$$

In momentum space the the shift operator is given by

$$S(k_x, k_y) = \begin{pmatrix} e^{ik_x} & 0 & 0 & 0 \\ 0 & e^{-ik_x} & 0 & 0 \\ 0 & 0 & e^{ik_y} & 0 \\ 0 & 0 & 0 & e^{-ik_y} \end{pmatrix}. \quad (15)$$

The walk then evolves by the recurrence relation $\hat{\Psi}(k_x, k_y, t + 1) = U^i(k_x, k_y)\hat{\Psi}(k_x, k_y, t)$ where $U^i(k_x, k_y) = S(k_x, k_y)C^i$ and C^i is the chosen coin operator. Therefore the walk evolves as $\hat{\Psi}(k_x, k_y, t) = U^i(k_x, k_y)^t \hat{\Psi}_0$ where $\hat{\Psi}_0 \equiv \hat{\Psi}(k_x, k_y, 0)$, and the walker is initially at the origin. For analytical purposes, instead of considering moments in terms of the radial distance from the origin we consider the joint moments which, for a two dimensional quantum walk, are given by

$$\begin{aligned} \langle X_t^\xi Y_t^\chi \rangle_\Psi &= \sum_{x,y \in \mathbb{Z}} x^\xi y^\chi \Psi^\dagger(x, y, t) \Psi(x, y, t) \\ &= \int_{-\pi}^{\pi} \int_{-\pi}^{\pi} \frac{dk_x dk_y}{(2\pi)^2} \hat{\Psi}^\dagger(k_x, k_y, t) \left(i \frac{\partial}{\partial k_x} \right)^\xi \left(i \frac{\partial}{\partial k_y} \right)^\chi \hat{\Psi}(k_x, k_y, t). \end{aligned} \quad (16)$$

where $i \frac{\partial}{\partial k_x}$ and $i \frac{\partial}{\partial k_y}$ are the momentum space representation of the position operators x and y . In order to calculate the state of the walker at time t for a particular C^i we

need to calculate the eigensystem of U^i . We will first of all take U^{1rep} and show that in this case the even moments, i.e., when $\xi + \chi$ is even, are independent of the initial state of the walker for large t . In Appendix A it is shown that the eigenvalues of $U^{1rep}(k_x, k_y)$ can be expressed as $\lambda_1 = e^{i\omega(k_x, k_y)}$, $\lambda_2 = -e^{i\omega(k_x, k_y)}$, $\lambda_3 = e^{-i\omega(k_x, k_y)}$, $\lambda_4 = -e^{-i\omega(k_x, k_y)}$ where ω is a function of k_x, k_y and all 8 coin parameters. We label a corresponding set of orthonormal eigenvectors by $|v_1(k_x, k_y)\rangle, |v_2(k_x, k_y)\rangle, |v_3(k_x, k_y)\rangle, |v_4(k_x, k_y)\rangle$. We will drop the k_x and k_y dependence from the notation. We may represent the state in terms of the eigensystem by

$$\hat{\Psi}(k_x, k_y, t) = U(k_x, k_y)^t \hat{\Psi}_0 = \sum_{j=1}^4 \lambda_j^t \langle v_j | \Psi_0 \rangle |v_j\rangle \quad (17)$$

We will now show that the joint moments as defined in Equation (16) are asymptotically independent of Ψ^0 using the method of Grimmett *et al.* to calculate the large t expression for the moments [16, 17]. First consider

$$\begin{aligned} \left(i \frac{\partial}{\partial k_x} \right)^\xi \left(i \frac{\partial}{\partial k_y} \right)^\chi \hat{\Psi}(k_x, k_y, t) &= \left(i \frac{\partial}{\partial k_x} \right)^\xi \left(i \frac{\partial}{\partial k_y} \right)^\chi \left\{ e^{i\omega t} (\langle v_1 | \Psi_0 \rangle |v_1\rangle + (-1)^t \langle v_2 | \Psi_0 \rangle |v_2\rangle) + e^{-i\omega t} (\langle v_3 | \Psi_0 \rangle |v_3\rangle + (-1)^t \langle v_4 | \Psi_0 \rangle |v_4\rangle) \right\} \\ &= e^{i\omega t} (\langle v_1 | \Psi_0 \rangle |v_1\rangle + (-1)^t \langle v_2 | \Psi_0 \rangle |v_2\rangle) (-t)^{\xi+\chi} \left(\frac{\partial \omega}{\partial k_x} \right)^\xi \left(\frac{\partial \omega}{\partial k_y} \right)^\chi \\ &\quad + e^{-i\omega t} (\langle v_3 | \Psi_0 \rangle |v_3\rangle + (-1)^t \langle v_4 | \Psi_0 \rangle |v_4\rangle) t^{\xi+\chi} \left(\frac{\partial \omega}{\partial k_x} \right)^\xi \left(\frac{\partial \omega}{\partial k_y} \right)^\chi + O(t^{\xi+\chi-1}) \end{aligned} \quad (18)$$

$$\hat{\Psi}^\dagger(k_x, k_y, t) \left(i \frac{\partial}{\partial k_x} \right)^\xi \left(i \frac{\partial}{\partial k_y} \right)^\chi \hat{\Psi}(k_x, k_y, t) = \{ (-1)^{\xi+\chi} \sum_{j=1}^2 |\langle v_j | \Psi_0 \rangle|^2 + \sum_{j=3}^4 |\langle v_j | \Psi_0 \rangle|^2 \} t^{\xi+\chi} \left(\frac{\partial \omega(k_x, k_y)}{\partial k_x} \right)^\xi \left(\frac{\partial \omega(k_x, k_y)}{\partial k_y} \right)^\chi + O(t^{\xi+\chi-1})$$

Now as $\sum_{j=1}^4 |\langle v_j | \Psi_0 \rangle|^2 = 1$ then if $\xi + \chi = 2n$, $n \in \mathbb{N}$ we have

$$\hat{\Psi}^\dagger(k_x, k_y, t) \left(i \frac{\partial}{\partial k_x} \right)^\xi \left(i \frac{\partial}{\partial k_y} \right)^\chi \hat{\Psi}(k_x, k_y, t) = t^{\xi+\chi} \left(\frac{\partial \omega(k_x, k_y)}{\partial k_x} \right)^\xi \left(\frac{\partial \omega(k_x, k_y)}{\partial k_y} \right)^\chi + O(t^{\xi+\chi-1}) \quad (19)$$

Therefore, by substituting Equation (19) into Equation (16) we see that under the condition $\xi + \chi = 2n$, and in the asymptotic limit of large t , the moments are independent of the initial state of the walker and are a function of the coin parameters only. From Appendix A it can be seen that the moments (asymptotically) depend only on the five parameters $m_1 = \alpha - \beta + \delta + \psi$, $m_2 = \phi + \delta$, $m_3 = \phi + \alpha - 2\theta + \psi + \beta$, λ and γ . This is because

$\omega(k_x, k_y)$ can be written as a function of $k_x, k_y, m_1, m_2, m_3, \lambda$ and γ . Although this is an asymptotic proof, numerical results show that this is true for any t , suggesting that the dependence on the initial states cancels in a similar way for all orders, not just the leading order.

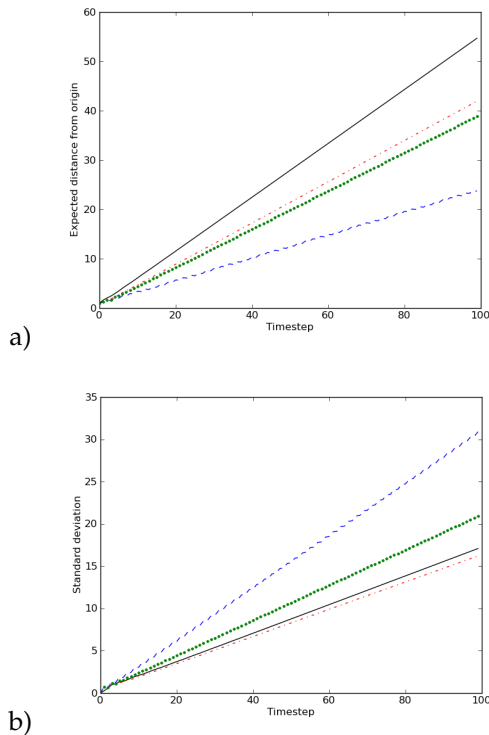


FIG. 5. (Color online) Comparison of the non-reversal (black line), Hadamard (red dots/dashes), Grover (blue dashes) and DFT (green dots) coin operators in terms of a) expected radial distance from the origin and b) standard deviation.

IV. THE NON-REVERSAL WALK

The result derived above applies only to walks using the operator U^{rep} . We conjecture that the same result holds for the non-reversal walk. As its eigensystem is not tractable, as shown in Appendix B, the non-reversal walk is treated numerically rather than analytically. These walks were investigated by varying the parameters in the coin as well as the initial condition. Random choices for each variable were used to generate 500 coins, and the walks arising from these operators were investigated using 1000 initial conditions. It was found numerically that for all choices of initial condition the mean position (Equation (1)) and standard deviation (Equation (2)) of the walker is constant at a given time t . Further investigations suggest that all the joint moments of the distribution where the x and y exponents sum to an even number are independent of the initial condition.

To compare with the non-repeating coin, we tested whether the moments were constant if the five parameters $m_1 = \alpha - \beta + \delta + \psi$, $m_2 = \phi + \delta$, $m_3 = \phi + \alpha - 2\theta + \psi + \beta$, λ and γ were held constant whilst varying their constituents. As in this case only twenty coins were tested, the results are not conclusive, but it appears that these same five parameters determine the moments in the case of the non-reversal coin.

The properties of both walks contrast strongly with those arising from previously studied coins, as mentioned in Section I B above, where the initial condition can be used to control the standard deviation of the walk using the Grover coin operator. The mean and standard deviations as a function of time are shown for a variety of coins, using the same initial condition for each, in Figure 5. Whilst the mean position increases faster than all other coins, the standard deviation increases more slowly, so in cases where we have freedom to choose our initial condition, the Grover operator is still the best to use if we want to achieve the fastest possible spreading of the amplitude across the lattice.

The analytics concerning the non-repeating coin deal with the joint moments, and numerical investigations of both coins showed that the individual x and y moments do depend on the initial condition. These were not investigated further as it appears that for practical applications of the model, the fully specified position of the walker will be of more interest.

V. CONCLUSION

We have introduced a new type of coin for the discrete time quantum walk and shown analytically, for one choice of shift operator, and numerically for the other, that it has some notable properties, namely that the mean and standard deviation of the radial distance from the origin of the walker is independent of the choice of initial condition. The standard deviation grows linearly with t for much the same reason as it does the walk on the line, as the coin operator always ensures that some amplitude moves away from the origin with each step. Further comparison was suggested by the analytical work, and we provide numerical evidence that the moments of the non-reversal walk depend on the same five parameters that determine those of the non-repeating walk. In both cases the individual x and y moments do depend on the initial condition of the walker.

A fully self-avoiding quantum walk is yet to be developed and explored, and thus far no continuous time analogues have been proposed. In order to fully capture the folding of polymer chains, the quantum nature of their constituents may need to be accounted for, which would provide a potential application for such a model.

In addition to further investigating the properties of the non-reversal quantum walk and developing the concept, better comparisons with its classical counterpart may be useful. For example, only walks on square lattices have been considered here, but the self-avoiding random walk has been shown to have macroscopic properties which are independent of the choice of lattice. In order to see if this property carries over into the quantum case, coins of varying dimension are required.

ACKNOWLEDGMENTS

KB is funded by the UK Engineering and Physical Sciences Research Council (EPSRC). VK is funded by a UK Royal Society Research Fellowship. TP, BH, and AB

received support from Royal Society summer bursaries and EPSRC. VP was supported by the International Association for the Exchange of Students for Technical Experience and SM by JFT Grant ID 15619 and ANR-10-JCJC-0208 CausaQ grant.

- [1] S. Gudder, *Quantum Probability*. Academic Press Inc., CA, USA, 1988.
- [2] Aharonov, Y., Davidovich, L., and Zagury, N., "Quantum random walks," *Phys. Rev. A*, vol. 2, p. 16871690, 1992.
- [3] G. Grossing and A. Zeilinger, "Quantum cellular automata," *Complex Systems*, vol. 2, p. 197 208, 1988.
- [4] A. Ambainis, E. Bach, A. Nayak, A. Vishwanath, and J. Vishwanath, "One-dimensional quantum walks," *Proc. 33rd Annual ACM STOC*, pp. 60–69, 2001.
- [5] J. Kempe, "Quantum random walks hit exponentially faster," *Probability Th. and Related Fields*, vol. 133 (2), p. 215235., 2005.
- [6] A. Childs, R. Cleve, E. Deotto, E. Farhi, S. Gutmann, and D. Spielman, "Exponential algorithmic speedup by quantum walk," in *Proc. 35th Annual ACM STOC*, pp. 59–68, 2003.
- [7] A. Childs, E. Farhi, and S. Gutmann, "An example of the difference between quantum and classical random walks," *Quantum Inf. Process.*, vol. 35, 2002.
- [8] M. Mohseni, P. Rebentrost, S. Lloyd, and A. Aspuru-Guzik, "Environment-assisted quantum walks in photosynthetic energy transfer," *J. Chem. Phys.*, no. 129, p. 174106, 2008.
- [9] B. Hayes, "How to avoid yourself," *AmSci*, vol. 86, p. 314, 1998.
- [10] I. Jensen, "A parallel algorithm for the enumeration of self-avoiding polygons on the square lattice," *J. Phys. A: Math. Gen.*, vol. 36, pp. 5731–5745, 2003.
- [11] A. J. Guttmann and A. R. Conway, "Square lattice self-avoiding walks and polygons," *Ann. Comb.*, vol. 5, pp. 319–345, 2001.
- [12] A. Skrilos and S. Chirikjian, "Position and orientation distributions for non-reversal random walks using space-group fourier transforms," *J Algebr Stat.*, vol. 1, pp. 27–46, 2010.
- [13] B. Tregenna, W. Flanagan, R. Maile, and V. Kendon, "Controlling discrete quantum walks: coins and initial states," *New J. Phys.*, vol. 5, no. 83, 2003.
- [14] T. D. Mackay, S. D. Bartlett, L. T. Stephenson, and B. C. Sanders, "Quantum walks in higher dimensions," *J. Phys. A: Math. Gen.*, vol. 35, 2002.
- [15] Kendon, V., "Quantum walks on general graphs," *Int. J. Quant. Inf.*, vol. 4(5), 2006.
- [16] G. Grimmett, S. Janson, and P. F. Scudo, "Weak limits for quantum random walks," *Physical Review E*, vol. 69, no. 2, p. 026119, 2004.
- [17] K. Watabe, N. Kobayashi, M. Katori, and N. Konno, "Limit distributions of two-dimensional quantum walks," *Physical Review A*, vol. 77, no. 6, p. 062331, 2008.

Appendix A

Here we calculate the eigenvalues of $U^{lrep}(k_x, k_y)$. Using algebraic manipulation software it can be shown that the characteristic equation for this matrix is given by

$$p^4 + 2p^2 \left(\gamma^2 \cos \Theta_1 - \lambda^2 \cos \Theta_2 - \cos \Theta_3 f(\lambda, \gamma)^2 \right) + 1 = 0$$

where $\Theta_1 = \alpha - \beta + \delta - k_y + \psi - k_x$, $\Theta_2 = \phi + \delta$ and $\Theta_3 = \phi + \alpha - 2\theta + k_y + \psi + \beta - k_x$. If we solve this equation for p we will obtain the 4 eigenvalues. As there are no first or third order terms in the characteristic equation, if p is a solution then so to is $-p$. As the coefficients are real then if p is a solution then so is p^* . As the coin is unitary we therefore have that the eigenvalues can be written as $\lambda_1 = e^{i\omega(k_x, k_y)}$, $\lambda_2 = -e^{i\omega(k_x, k_y)}$, $\lambda_3 = e^{-i\omega(k_x, k_y)}$, $\lambda_4 = -e^{-i\omega(k_x, k_y)}$ where ω is a function of λ , γ , Θ_1 , Θ_2 , and Θ_3 and so hence is a function of k_x, k_y and all 8 coin parameters. By solving the effective quadratic it can be shown that the solutions are given by $\lambda_i = \pm_s \sqrt{a_r \pm_t ia_i}$, where the subscripts denote that the \pm s are independent and $a_r = -b$, $a_i = \left| \sqrt{b^2 - 1} \right|$, $b = \gamma^2 \cos \Theta_1 - \lambda^2 \cos \Theta_2 - \cos \Theta_3 f(\lambda, \gamma)^2$.

Appendix B

The characteristic equation for U^{lrev} can be shown to be

$$p^4 + \Delta p^3 + \Xi p^2 + \Delta^* p + 1 = 0$$

where $\Delta = -\lambda \left(e^{i(\alpha - k_x)} + e^{i(k_x - \phi - \delta - \alpha)} + e^{i(\phi - k_y)} + e^{i(\delta + k_y)} \right)$ and $\Xi = 2(\cos(\phi + \alpha - k_y - k_x)(1 - \gamma^2) + \cos(\delta + \alpha + k_y - k_x)(\lambda^2 + \gamma^2) + \lambda^2 \cos(\phi + \delta))$. This quartic does not in general have the properties of that in appendix A. However if $\delta = -\phi$ then $\Delta = \Delta^*$ and so the characteristic equation is quasi-symmetric and has real parameters. As the parameters are real, if p is a solution then so is p^* . It can be shown that the solutions are not of the required form (i.e. $p = e^{i\omega}$). Instead they are of the form

$$p = -\frac{\Delta}{2} \pm_s \frac{\sqrt{\Delta^2 - 4(\Xi - 2)}}{2} \pm_t \frac{\sqrt{2\Delta^2 - 4(\Xi + 2) \mp_s \Delta \sqrt{\Delta^2 - 4(\Xi - 2)}}}{4}$$

and the proof method for U^{rep} does not follow for U^{rev} .